pH Dependent Concatenation of an Inorganic Complex Results in Solid State Helix Formation

Emily Hoffer,[a] Brian P. Niebuhr,[a] Kristof Pota,[a] Timothy M. Schwartz,[a] Marianne E. Burnett,[a] Timothy J. Prior,[b] Horst Puschmann,[c] Kayla N. Green[a,*]

[a.] *Department of Chemistry and Biochemistry, Texas Christian University, 2950 S. Bowie, Fort Worth, TX 76129, United States*
[b.] *Department of Chemistry, University of Hull, Cottingham Road, Hull HU6 7RX, UK.*
[c.] *OlexSys Ltd, Chemistry Department, Durham University, DH1 1LA, UK*

Growth of the library of tetraaza macrocyclic pyridinophane ligands is a result of the potential to treat neurodegenerative diseases by binding unregulated redox active metal-ions, scavenging radicals, and reducing oxidative stress. As part of this work, the copper complex of **^{OH}PyN$_3$Cu** (3,6,9,15-tetraazabicyclo[9.3.1]penta-deca-1(15),11,13-trien-13-ol) was previously identified as a discrete molecule in the solid state when isolated at lower pH values. However, here we report that **^{OH}PyN$_3$Cu** forms a helical structure upon crystallization around pH 6.5. Several properties of the ligand and complex were evaluated to understand the driving forces that led to the concatenation and formation of this solid-state helix. DFT studies along with a comparison of keto/enol tautomerization stability and bond lengths were used to determine the keto-character of the C=O within each subunit. This pH dependent keto-enol tautomerization is responsible for the solid state intermolecular C=O···Cu bonds observed in this metallohelix (**Cu1$_H$**) when produced around pH 6.5. Perchlorate templating that occurs through hydrogen bonding between perchlorate counter ions and each **Cu1$_H$** unit is the primary driving factor for the twist that leads to the helix structure. **Cu1$_H$** does not exhibit the typical factors that stabilize the formation of helices, such as intra-strand hydrogen bonding or π-stacking. The helix structure further highlights the diversity of inorganic metallohelices and demonstrates the importance of tautomerization and pH that occurs with the pyridinophane ligand used in this study. To our knowledge and although these phenomenon have been observed individually, this is the first example of a pH dependent keto-enol tautomerization in an azamacrocycle being the driving force for the formation of a metallohelix solid state structure and is a particularly unique observation for pyridinophane complexes.

Introduction

Helices are three-dimensional structures that often result from inter- and intramolecular forces within a molecule or molecules. These unique assemblies serve as critical components for many biological structures; the best-known examples include the double helix of DNA and the many derivatives of

alpha helices in protein backbones. Aside from the biological importance of helices, metallohelices have been widely reported in the literature and serve a variety of purposes.[1-5] For example, a thymidine helix structure was designed by Roth and coworkers to enhance enantioselective recognition processes (Figure 1a).[2] Dey and coworkers reported a helix composed of a copper(II) complex with syn- and anti-carboxylate bridges (Figure 1b).[3] Moreover, Lehn and coworkers reported that oligobipyridine ligands and copper(I) spontaneously formed a double-stranded helicate with the copper(I) cations at the center of the structure.[4] This system offered the opportunity for further studies focused on the self-organization, cooperativity, and chirality within a helix, applications to organic and inorganic chemistry, as well as the potential ability to bind and cleave DNA with specialized selectivity. Some metallohelices have proven biological applications. For example, the solid-state structure of the antiarthritic drug gold thiomalate was reported to form a double helix (Figure 1c).[5]

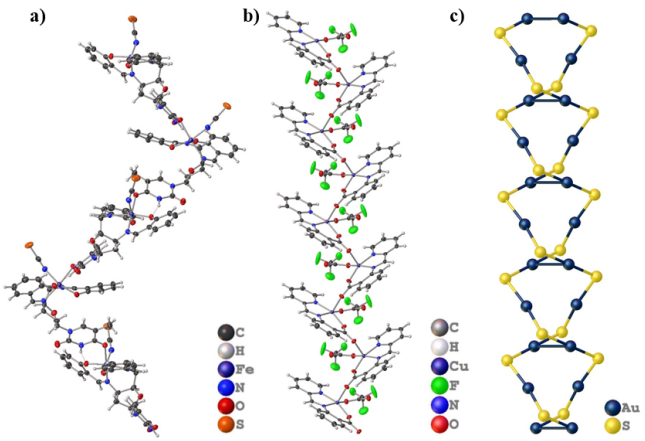

Figure 1. Representative examples of metallohelices reported to date. **a)** Thymidine chiral helix,[2] **b)** Copper (II) complex with syn- and anti-carboxylate bridges helix,[3] **c)** Thiomalate double helix with the helix Au-S core shown.[5]

We have reported a library of tetraaza macrocyclic pyridinophane ligands with the potential to target the oxidative stress associated with the development of neurodegenerative diseases such as Alzheimer's. The copper(II) complex of the tetraaza pyridinophane ^{OH}**PyN$_3$** (**1** = 3,6,9,15-tetraazabicyclo[9.3.1]penta-deca-1(15),11,13-trien-13-ol) (Figure 2), has been shown to have enhanced antioxidant capabilities compared to parent macrocyclic structures such as cyclen and pyclen derived molecules. Biological and pharmacological studies of **1** suggest that it could have positive therapeutic effects against neurodegenerative diseases.[6-8] In our original report, we observed

a mononuclear, pentacoordinate copper complex (**Cu1$_M$**, Figures 2a-b).[8] As a result of a recent re-visitation to this work and using a modified procedure, copper(II) complexes of **1** were observed to form crystals with a helix structure (**Cu1$_H$**, Figures 2c-e) when produced at pH values higher (pH~6.5) than those used previously. Here we present the study of **Cu1$_H$** helical structure and relate the results to potentiometric studies and DFT to show that the formation of the helix is correlated to the pH-dependent keto-enol tautomerization of the ligand.

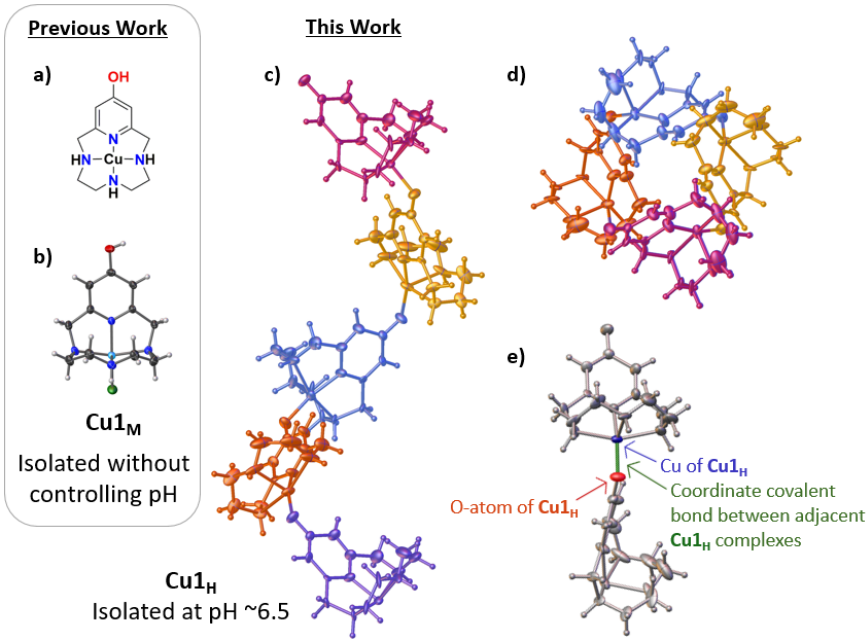

Figure 2. a) Drawing of **Cu1**. **b)** Solid State structure previously reported[8] for **Cu1$_M$. c)** View of the **Cu1$_H$** helix from the side, depicting five **Cu1$_H$** units. **d)** View of **Cu1$_H$** helix **down the crystallographic *c* axis**, which highlights that each rotation is composed of four **Cu1$_H$** units, evidenced by the complete overlap of the first **Cu1$_H$** unit (pink) with the fifth **Cu1$_H$** unit (violet). **e)** A coordinate covalent bond between the copper(II) of one **Cu1** complex and the O-atom of an adjacent **Cu1** complex connects the units to form the helix structure.

Results and Discussion

We have previously reported that monomeric copper(II) complexes of **Cu1** are obtained by the addition of copper(II) perchlorate to a solution of the hydrochloride salt of ligand **1** in water at an initial pH 7.[8] Using this method, the pH of the solution drops to 2-3 after stirring overnight, but the copper(II) complex (Figure 2a-b) forms in good yields. X-ray diffraction analysis of single crystals, obtained by slow evaporation, showed discrete monomeric **Cu1$_M$** complexes in solution and in the

solid state. Each copper(II) ion was bound to the four N-atoms of the pyridinophane macrocycle with a chloride ion as a fifth coordinating ligand. The hydroxyl group on the 4-position of the pyridine ring displayed a hydrogen bond to the adjacent perchlorate counter ion, but no other interactions were observed between **Cu1$_M$** units. However, a markedly different solid-state structure was observed when this procedure was repeated but with continued adjustment of the pH to roughly 6.5. Blue single crystals were obtained by slow evaporation of the aqueous mother liquor. Analysis using X-ray diffraction at 100 K resulted in the model shown in Figures 2c-e. The helical nature of the **Cu1$_H$** structure is evident when viewed down the crystallographic *c* axis. Four concatenated **Cu1** units are required to complete one full rotation of this right-handed helix, which is composed of a **Cu1** consecutively connected through a coordinate covalent bond between the O-atom of the ligand **1** with the copper(II) ion of the adjacent **Cu1$_H$** complex (Figure 2e). Perchlorate anions are disordered throughout, which complicates the structural analysis. Each perchlorate occupies two different orientations related by 180° rotation in equal amounts and this is a consequence of the high symmetry space group; each chloride resides on a 4*a* Wyckoff position with site symmetry (..2). There are N-H···O interactions observed between the helices and the perchlorate counter ions, which reside in the groove formed from turns in the helix (Figure 3). A packing diagram reveals the groove of one helix unit interlocks with the curve of an adjacent helix (Figure 3b-c). This interdigitation of adjacent helices is a phenomenon that has been observed to stabilize microporous chiral molecular frameworks in previous studies and will be described further below.[9]

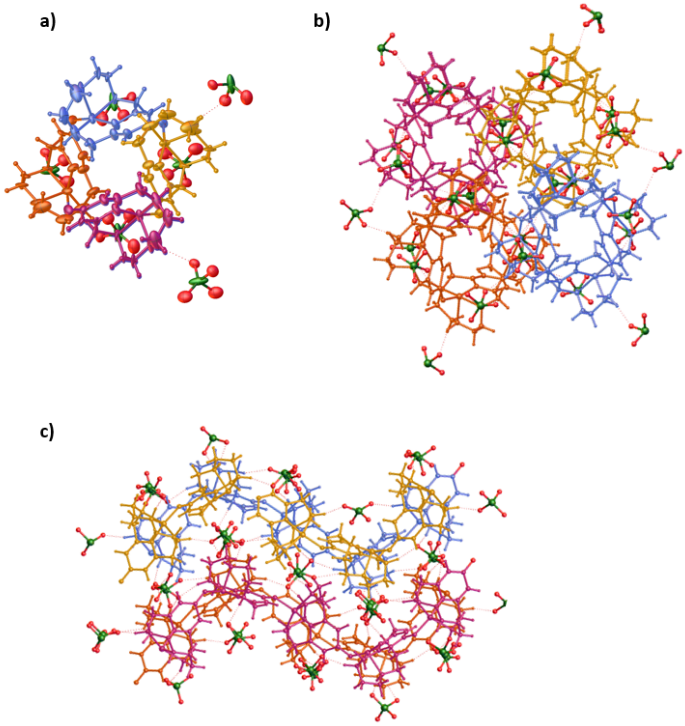

Figure 3. a) View of **Cu1$_H$** helix down the crystallographic *c* axis with perchlorate counter ions. b) View down the crystallographic *c* axis of four strands of **Cu1$_H$** packed, including perchlorate counter ions. c) View along the *a* axis of four strand of **Cu1$_H$** packed, including perchlorate counter ions.

We hypothesized that the pH of the solution during complexation and crystallization was responsible for the modulated speciation of the **Cu1** complex between the mononuclear complex observed previously and this newly observed helix in the crystalline form. This is supported by several observations. Ligand **1** undergoes a keto-enol tautomerization, favoring the keto form between pH values of 5.45 – 9.0.[6] Likewise, the **Cu1** complex also undergoes a protonation event in a similar pH range (Scheme 1, Figure 4). For comparison, while the enol tautomer was observed to be more stable than the keto form of the dianionic form of chelidamic acid (**2**$^{2-}$), the keto tautomer was preferred with the **2Me$_2$** congener (Figure 5).[10, 11] The shift in preference for enol vs. keto is due to the methyl ester being more electron-withdrawing than the deprotonated carboxyl. Therefore, it is reasonable to consider that the copper(II) cation of **Cu1** has an electron-withdrawing effect on the pyridol ring, which would similarly stabilize the keto form of the complex. The deprotonation of the **Cu1** complex creates the opportunity for the oxygen bridge to form between each unit, and the strand becomes the thermodynamically favored structure over the monomeric unit. Furthermore, inspection of the bond lengths within the solid-state structure of **Cu1$_H$** support that the keto tautomer is prevalent. The C-O bond length (1.28(3) Å) lies more closely to the keto form of [**2Me$_2$**] (1.274 Å) compared to the enol form of [**2**$^{2-}$] (1.331 Å) and monomeric **Cu1$_M$** (1.340 Å) (Figure 6). [8, 12-14]

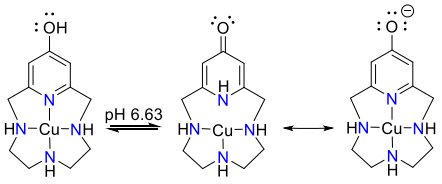

Scheme 1. Keto-enol tautomerization of **Cu1**. [6]

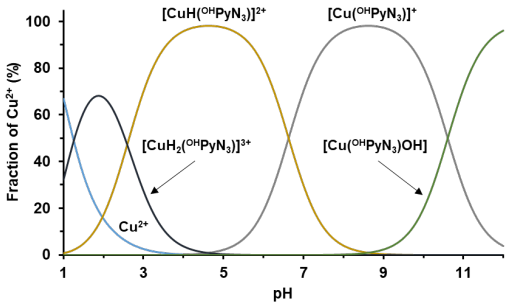

Figure 4. Equilibrium distribution diagram of the Cu(II)-^{OH}**PyN$_3$** system.[6]

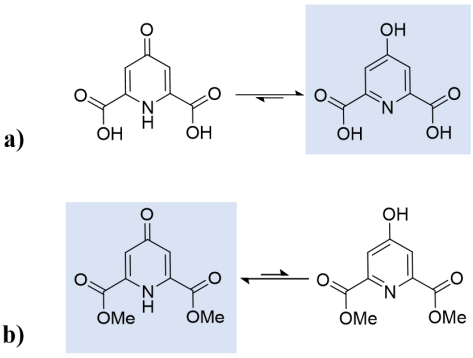

Figure 5. a) The enol tautomer of chelidamic acid [**2**$^{2-}$] is more stable than the keto tautomer. b) When electron-withdrawing methyl ester groups replace the carboxylate groups [**2Me$_2$**], the keto tautomer is more stable than the enol tautomer.

Additionally, DFT analysis was used to determine whether the keto or enol tautomer was preferred in the solid state. **Cu1$_H$** was modeled with a coordinated aqua ligand, using wB97XD[15] with the 6-31+g(d,p)[16] basis set and a water SMD[17] solvent model. First, the relaxed geometry was determined, followed by fixing the C-O bond length to specific lengths. The fixed bond lengths chosen were 1.2736 Å, 1.298 Å, and 1.349 Å. These correspond to the bond lengths found in the crystal structures of 4-pyridone[18, 19], **Cu1$_H$**, and 4-nitrophenol[20], respectively. The 4-pyridone bond length was chosen as the model for the keto form because it exhibits a preference for the keto tautomer. The 4-nitrophenol bond length was chosen as the model for the enol form because the electronics of pyridine or more akin to nitrobenzene. Therefore, the 4-nitrophenol bond length is more applicable than phenol itself. Each model had no imaginary frequencies.

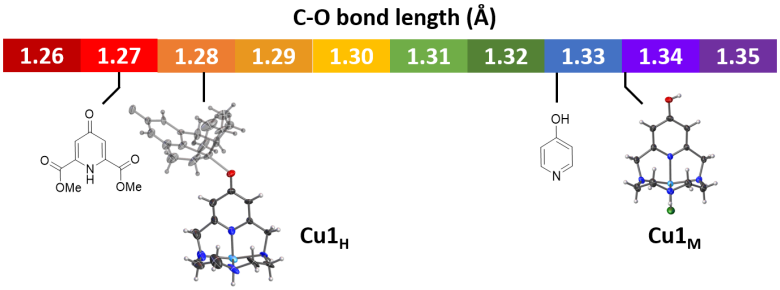

Figure 6. Comparison of C-O bond lengths reveals that the C-O bond length in **Cu1$_H$** is close to the C-O bond length in the keto form of **2Me$_2$**.

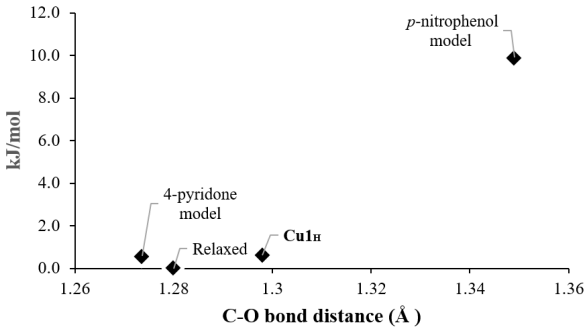

Figure 7. Energy values of **Cu1$_H$** with fixed bond lengths, corresponding to the bond length of 4-pyridone[18, 19], the solid-state structure of **Cu1$_H$**, and the bond length of *p*-nitrophenol[20], all relative to the relaxed geometry.

As shown in Figure 7, the energy values of each fixed bond length were compared to the relaxed geometry, which was found to have a bond length of 1.28 Å. The enol congener had a much higher energy of 9.90 kJ/mol, while the keto congener had an energy of 0.572 kJ/mol, both relative to the relaxed geometry. The solid-state bond length in **Cu1$_H$** is much closer to both the relaxed and keto geometries, with an energy of 0.627 kJ/mol, relative to the relaxed geometry. Based on the XRD and DFT data, **Cu1$_H$** can be assigned as the keto tautomer. We propose then that the bond order between the carbon-oxygen atoms is closer to two, containing both sigma and pi-electrons. The unique character of the keto-tautomer gives rise to the O···Cu intermolecular bridge that results in the formation of the unique helix observed.

Having established that the **Cu1$_H$···O** interaction was facilitated by the keto form of the **^{OH}PyN$_3$Cu** complex, we set out to determine what properties further facilitated the helical structure observed in the solid state. It is important to note that dissolution of crystals of **Cu1$_H$** result in breaking of the helix lattice and formation of discrete monomeric species based on UV-vis and potentiometric studies. Common interactions that typically lead to helix formation were not observed for **Cu1$_H$**. The **Cu1$_H$** helix is single-stranded and, therefore, cannot be stabilized by hydrogen bonding between two strands as is observed in structure like DNA. Furthermore, no evidence of *intramolecular* hydrogen bonding within **Cu1$_H$** is observed that would stabilize the conformation. Likewise, there is no evidence of π-π stacking between the pyridine rings within one helix or between adjacent helices. The closest contacts observed were between the H-atom on N4 and H4 of the adjacent **Cu1$_H$** unit (Figure 8). One previous example of a metallohelix reported by Lehn and coworkers was stabilized by the presence of cations at the center of the helix.[4] Although our helix contains the copper(II) cation, these cations are located within the strand and do not provide a framework for our ligand to surround.

Although the copper(II) cations cannot provide a framework for the helix, analysis of the packing of the strands and counter ions indicates that perchlorate templating is the probable driving force for the formation of the helical structure. This is achieved through the resulting hydrogen bonds between the strands of connected complexes. The ability of perchlorate ions to template or stabilize the formation of helical three-dimensional structures from polymers, such as peptides, has been reported in the literature.[21] However, to our knowledge perchlorate templating has not yet been observed to facilitate helix formation in structures such as **Cu1$_H$** or other macrocycles that are typically isolated as independent units in the solid state. For **Cu1$_H$** , each perchlorate ion is found in a "pocket" of the helix and forms N-H···O hydrogen bonds to adjacent strands of **Cu1$_H$** (Figure 8).

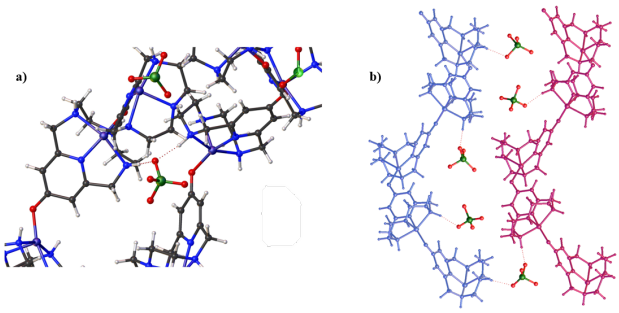

Figure 8. a) N-H···O hydrogen bonding occurs between an oxygen atom of perchlorate and a hydrogen atom of **Cu1$_H$**. b) Perchlorate ions between two strands of **Cu1$_H$**. The ions are found along the interior curve of the helix.

A slight asymmetry within each **Cu1$_H$** unit is observed. This is in contrast to the mirror plane identified from the hydroxyl moiety through the copper(II) ion of **Cu1$_M$**.[8] The degree of the twist in the ligand of **Cu1$_H$** is evident with the positions of the C-atoms alpha to the pyridine ring. This can be estimated by comparing the twist in the planes formed between C1C2C3N1 (177(2)°) and C2C3C4N1 (174(2)°) (Figure 9). The side of the molecule with the larger angle is located in the interior of the helix rotation and the N-atom forms a hydrogen bond to one of the perchlorate ions in the helix groove (Figure 8). Conversely, the opposite plane is located on the exterior side of the helix with no hydrogen bonds observed. The presence of hydrogen bonding to the perchlorate ions creates this asymmetry and this interaction pulls the interior side of **Cu1$_H$** toward the perchlorate ion, thereby creating the rotation necessary for a strand of **Cu1$_H$** to twist into the helix conformation.

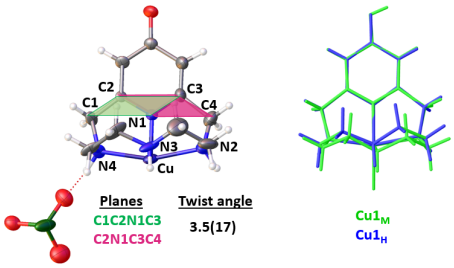

Figure 9. Twist angles for **Cu1$_H$** (left) and overlay of **Cu1$_M$** vs**. Cu1$_H$** (right) highlighting the asymmetry of the **Cu1$_H$** complex compared to **Cu1$_M$**.

Experimental

General Methods

Methanol was distilled from KOH and stored over 4Å molecular sieves. Other solvents and chemicals were purchased from commercial sources and used as received. A Leica MZ 75 microscope was used to identify samples suitable for analysis. A Bruker APEX-II CCD diffractometer was employed for crystal screening, unit cell determination, and data collection, which were obtained at 100 K. The Bruker D8 goniometer was controlled using the APEX3 software suite.[22] The samples were optically centered with the aid of a video camera so that no translations were observed as the crystal was rotated through all positions. The X-ray radiation employed was generated from a Mo Kα sealed X-ray tube (λ = 0.71076 Å) with a potential of 50 kV and a current of 30 mA, fitted with a graphite monochromator in the parallel mode (175 mm collimator with 0.5 mm pinholes). A full matrix least squares refinement based on F^2 was carried out within the Olex2[23] using SHEXL-2018[24, 25]. All hydrogen and non-hydrogen atoms were refined using anisotropic thermal parameters. CrysAlisPro 1.171.41.31a (Rigaku Oxford Diffraction, 2019) was used for empirical absorption correction using spherical harmonics, implemented in SCALE3 ABSPACK scaling algorithm. The thermal ellipsoid molecular plots (50%) were produced using Olex2.[23]

Synthesis of Cu1$_H$. Ligand **1** was prepared according to a previous report.[8] The copper complex was prepared in accordance with the same report but with monitoring the pH using a pH probe. The pH was adjusted to 6.5±0.3 using NaOH(aq), which needed to be repeated every few hours. The reaction was considered complete when the pH no longer changed. The solution was filtered and allowed to slowly evaporate and form crystalline material that was used for the analysis herein.

X-ray diffraction analysis. Cu1$_H$ crystallized as aggregates of blocks from an aqueous solution. All of the crystals examined were found to be multiple crystals. The crystal examined showed the presence

of a single dominant domain, but the diffraction data were still contaminated by the presence of at least one other domain. The nature of the overlap of spots from the two principal domains precluded de-twinning of the data and it was not possible to carry out multi-domain integration of the data. We hope to return to this problem in the future after further recrystallizations from a wide variety of different solvents. The data from the principal domain are of acceptable quality (R_{int} = 0.1391) and we have used these to solve the structure. Initially the structure was solved by dual-space methods in the orthorhombic space group $P2_12_12_1$. However, PLATON revealed additional symmetry was present and the structure was transformed to $P4_32_12$. Satisfactory refinement of the structure as a racemic twin (Flack parameter 0.010(12) (Parson's method) was possible and this yielded a straightforward determination of the structure that confirmed the atomic connectivity. Due to the nature of the crystal examined the quality of fit parameters are not particularly good but this does not change the soundness of the determination of the atomic arrangement.

Conclusions

X-ray diffraction showed that the **Cu1** complex forms a single-stranded helix when crystallized at a pH around 6.5. We have shown that the solution pH plays an important role in the speciation of the $\mathbf{Cu1_H}$ complex. Based on potentiometric data[26], a deprotonation event occurs at pH 6.63. DFT, XRD analysis, and comparison to previously reported compounds supports that this protonation results in a transition from the enol to keto tautomer within the complex. It should be noted that helix formation could not be replicated at higher pH values or with other counter ions. While the enol tautomer is observed at more acidic pH and results in a discrete complex in the solid state[8], the keto form facilitates a coordinate covalent bond between the copper(II) ion of one **Cu1** complex and the O-atom of an adjacent **Cu1** complex. Classic hydrogen bonding or π-stacking associated with many helix structures were not observed within $\mathbf{Cu1_H}$. Rather, intermolecular hydrogen bonding between perchlorate counter ions and $\mathbf{Cu1_H}$ units yield a slight asymmetry that is responsible for the rotation of the three-dimensional helix structure. To the best of our knowledge, this represents the first example of a metallohelix derived from a macrocyclic complex and represents a unique example where pH controls monomeric vs. oligomer type solid state structures.

Author Contributions

The manuscript was written through contributions of all authors. All authors have given approval to the final version of the manuscript.

Conflicts of interest

There are no conflicts to declare.

AUTHOR INFORMATION

Corresponding Author: kayla.green@tcu.edu

Acknowledgements

The authors acknowledge the TCU High-Performance Computing Center for providing HPC resources and the Welch Foundation (23770 to K.N.G.) for funding.

References

1. C. Gieck and W. Tremel, Interlocking Inorganic Screw Helices: Synthesis, Structure, and Magnetism of theNovelFrameworkUraniumOrthothiophoshatesA11U7(PS4)13 (A K,Rb) *Chem. Eur. J.*, 2002, **8**(*13*) 2980-2987.
2. A. Roth, D. Koth, M. Gottschaldt and W. Plass, An Inorganic Thymidine Helix: Design of Homochiral Helical Arrays, *Crystal Growth & Design*, 2006, **6**, 2655-2657.
3. S. K. Dey, B. Bag, K. M. Abdul Malik, M. S. El Fallah, J. Ribas and S. Mitra, A Quasi-Tetrahedral Cu4Cluster and a Helical-Chain Copper(II) Complex with Single Syn−Anti Carboxylate Bridges: Crystal Structure and Magnetic Properties, *Inorganic Chemistry*, 2003, **42**, 4029-4035.
4. J. M. Lehn, A. Rigault, J. Siegel, J. Harrowfield, B. Chevrier and D. Moras, Spontaneous assembly of double-stranded helicates from oligobipyridine ligands and copper(I) cations: structure of an inorganic double helix, *Proceedings of the National Academy of Sciences*, 1987, **84**, 2565-2569.
5. R. Bau, Crystal Structure of the Antiarthritic Drug Gold Thiomalate (Myochrysine): A Double-Helical Geometry in the Solid State, *Journal of the American Chemical Society*, 1998, **120**, 9380-9381.
6. K. N. Green, K. Pota, G. Tircsó, R. A. Gogolák, O. Kinsinger, C. Davda, K. Blain, S. M. Brewer, P. Gonzalez, H. M. Johnston and G. Akkaraju, Dialing in on pharmacological features for a therapeutic antioxidant small molecule, *Dalton Transactions*, 2019, **48**, 12430-12439.
7. H. M. Johnston, K. Pota, M. M. Barnett, O. Kinsinger, P. Braden, T. M. Schwartz, E. Hoffer, N. Sadagopan, N. Nguyen, Y. Yu, P. Gonzalez, G. Tircsó, H. Wu, G. Akkaraju, M. J. Chumley and K. N. Green, Enhancement of the Antioxidant Activity and Neurotherapeutic Features through Pyridol Addition to Tetraazamacrocyclic Molecules, *Inorg. Chem.*, 2019, **58**, 16771-16784.
8. K. M. Lincoln, P. Gonzalez, T. E. Richardson, D. A. Julovich, R. Saunders, J. W. Simpkins and K. N. Green, A potent antioxidant small molecule aimed at targeting metal-based oxidative stress in neurodegenerative disorders, *Chemical Communications*, 2013, **49**, 2712-2714.
9. C. J. Kepert, T. J. Prior and M. J. Rosseinsky, A Versatile Family of Interconvertible Microporous Chiral Molecular Frameworks: The First Example of Ligand Control of Network Chirality, *J. Am. Chem. Soc.*, 2000, **122**, 5158-5168.
10. M. Tutughamiarso, T. Pisternick and E. Egert, Pseudopolymorphs of chelidamic acid and its dimethyl ester, *Acta Crystallographica Section C*, 2012, **68**, o344-o350.
11. I. Alkorta and J. Elguero, A density functional theoretical study of the influence of cavities and water molecules on tautomerism: The case of pyridones and 1,2,4-triazoles linked to crown ethers and esters, *Journal of Heterocyclic Chemistry*, 2001, **38**, 1387-1391.
12. A. K. Hall, J. M. Harrowfield, B. W. Skelton and A. H. White, Chelidamic acid monohydrate: the proton complex of a multidentate ligand, *Acta Crystallographica Section C*, 2000, **56**, 448-450.
13. H. Aghabozorg, N. Firoozi, L. Roshan, H. Eshtiagh-Hosseini, A. R. Salimi, M. Mirzaei, M. Ghanbari, M. Shamsipur and M. Ghadermazid, Supramolecular structure of calcium(II) based on chelidamic acid: An agreement between theoretical and experimental studies, *Journal of the Iranian Chemical Society*, 2011, **8**, 992-1005.
14. K. M. Lincoln, M. E. Offutt, T. D. Hayden, R. E. Saunders and K. N. Green, Structural, Spectral, and Electrochemical Properties of Nickel(II), Copper(II), and Zinc(II) Complexes Containing 12-Membered Pyridine- and Pyridol-Based Tetra-aza Macrocycles, *Inorg. Chem.*, 2014, **53**, 1406-1416.
15. J.-D. Chai and M. Head-Gordon, Long-range corrected hybrid density functionals with damped atom–atom dispersion corrections, *Physical Chemistry Chemical Physics*, 2008, **10**, 6615-6620.

16. G. A. Petersson, A. Bennett, T. G. Tensfeldt, M. A. Al-Laham, W. A. Shirley and J. Mantzaris, A complete basis set model chemistry. I. The total energies of closed-shell atoms and hydrides of the first-row elements, *The Journal of Chemical Physics*, 1988, **89**, 2193-2218.
17. A. V. Marenich, C. J. Cramer and D. G. Truhlar, Universal Solvation Model Based on Solute Electron Density and on a Continuum Model of the Solvent Defined by the Bulk Dielectric Constant and Atomic Surface Tensions, *The Journal of Physical Chemistry B*, 2009, **113**, 6378-6396.
18. A. Tyl, M. Nowak and J. Kusz, Two polymorphs of anhydrous 4-pyridone at 100 K, *Acta Cryst.*, 2008, **C64**, 661-664.
19. H. T. Flakus and A. Tyl, Electron-induced phase transition in hydrogen-bonded anhydrous solid state 4-pyridone, *Vibrational Spectroscopy*, 2012, **63**, 440-450.
20. G. Wójcik and I. Mossakowska, Polymorphs of p-nitrophenol as studied by variable-temperature X-ray diffraction and calorimetry: comparison with m-nitrophenol, *Acta Cryst.*, 2006, **B62**, 143-152.
21. W. Maison, R. J. Kennedy and D. S. Kemp, Chaotropic Anions Strongly Stabilize Short, N-Capped Uncharged Peptide Helicies: A New Look at the Perchlorate Effect, *Angewandte Chemie International Edition*, 2001, **40**, 3819-3821.
22. Bruker-Nano, APEX3 : Suite for Crystallographic Software. Single Crystal.*Journal*, 2019, Suite for Crystallographic Software. Single Crystal.
23. O. V. Dolomanov, L. J. Bourhis, R. J. Gildea, J. A. K. Howard and H. Puschmann, OLEX2: a complete structure soluiton, refinement and analysis program, *J. Appl. Cryst.*, 2009, **42**, 339-341.
24. G. M. Sheldrick, Crystal structure refinement with SHELXL, *Acta Cryst.*, 2015, **C71**, 3-8.
25. G. M. Sheldrick, A short history of SHELX, *Acta Cryst.* , 2008, **A64**, 112-122.
26. K. N. Green, K. Pota, G. Tircsó, R. A. Gogolák, O. Kinsinger, C. Davda, K. Blain, S. M. Brewer, P. Gonzalez, H. M. Johnston and G. Akkaraju, Dialing in on pharmacological features for a therapeutic antioxidant small molecule, *Dalton Trans.*, 2019, **48**, 12430-12439.

Table of Contents Figure